Electronic Supplementary Material (ESI) for Journal of Materials Chemistry A.


# Enhanced performance of doped BiOCl nanoplates for photocatalysis: understanding from the doping insight into the improved spatial carriers separation

Wenwen Liu,[a] Yanyang Shang,[a] Anquan Zhu,[a] Pengfei Tan,[a] Yi Liu,[a] LuLu Qiao,[a] Dewei Chu,[b] Xiang Xiong [a] and Jun Pan* [a]

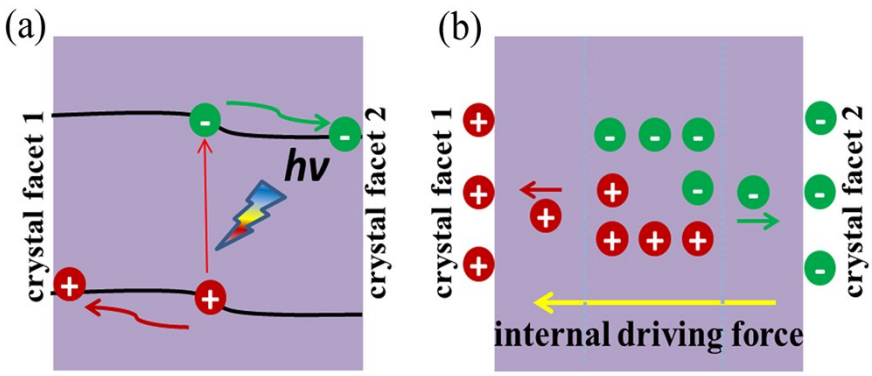


**Figure S1.** Schematic illustration for spatial separation of photoexcited carriers.

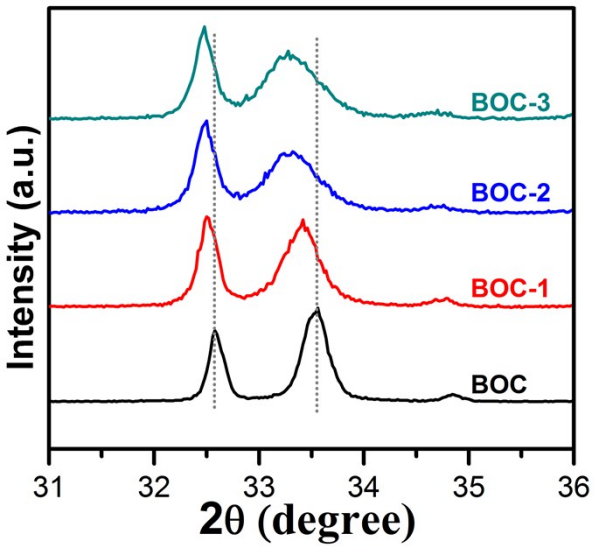


**Figure S2.** XRD magnified patterns of BOC, BOC-1, BOC-2 and BOC-3.

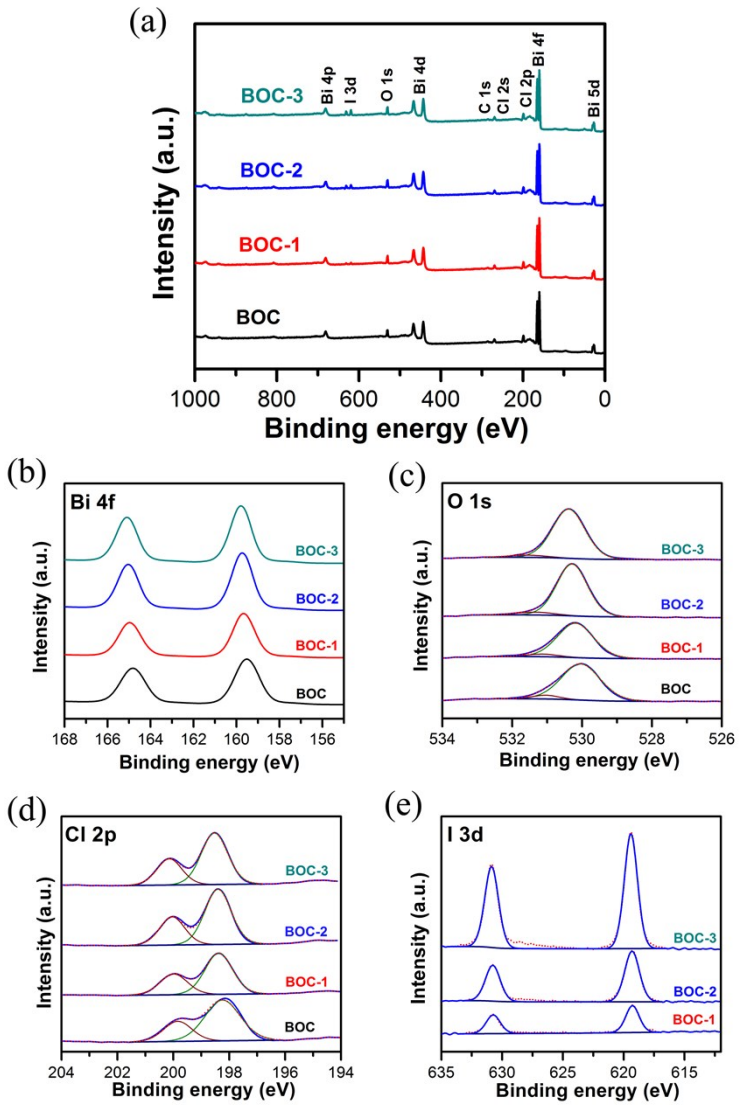


**Figure S3.** XPS of BOC, BOC-1, BOC-2 and BOC-3.

The compositions of as prepared BOC, BOC-1, BOC-2 and BOC-3 were investigated by XPS analysis. The survey spectra shown in **Figure S3a** indicate that iodine is detected in doped BiOCl nanoplates besides Bi, O, Cl and C. The C1s peak at around 284.8 eV can be attributed to the signal from instrument referencing. **Figure S2b-2e** shows the high-resolution XPS spectra of Bi 4f, O 1s, Cl 2p and I 3d, which are related to Bi-O bonds in $[Bi_2O_2]^{2+}$ slabs, lattice oxygen in $[Bi_2O_2]^{2+}$ slabs, $Cl^-$ and $I^-$ in doped BiOCl nanoplates, respectively. Iodine dopant concentration of BOC, BOC-1, BOC-2 and BOC-3 can be indexed to 0, 0.72%, 1.81% and 3.05%, respectively, as shown in **Table S1.**

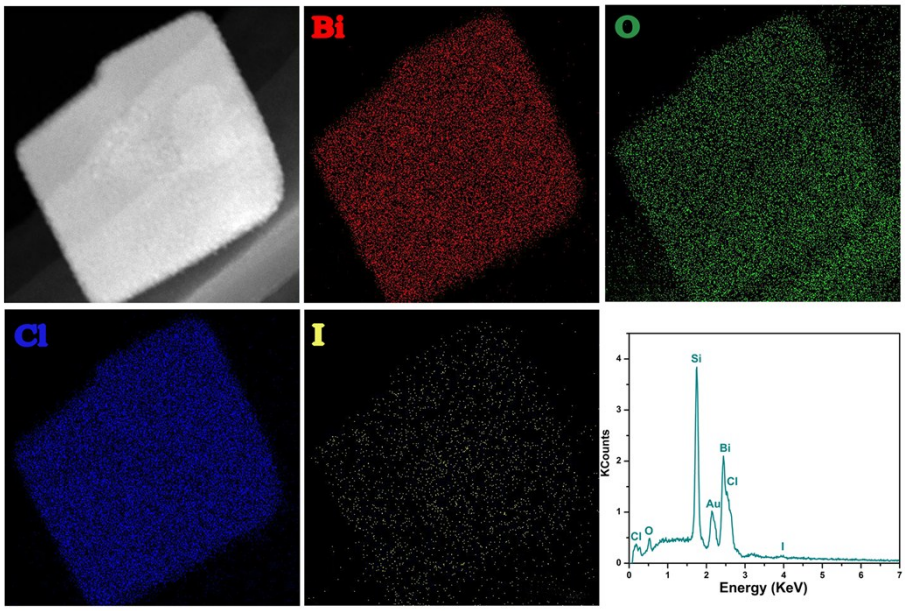


**Figure S4.** HAADF-STEM and corresponding elemental mapping images as well as EDS pattern of BOC-3.

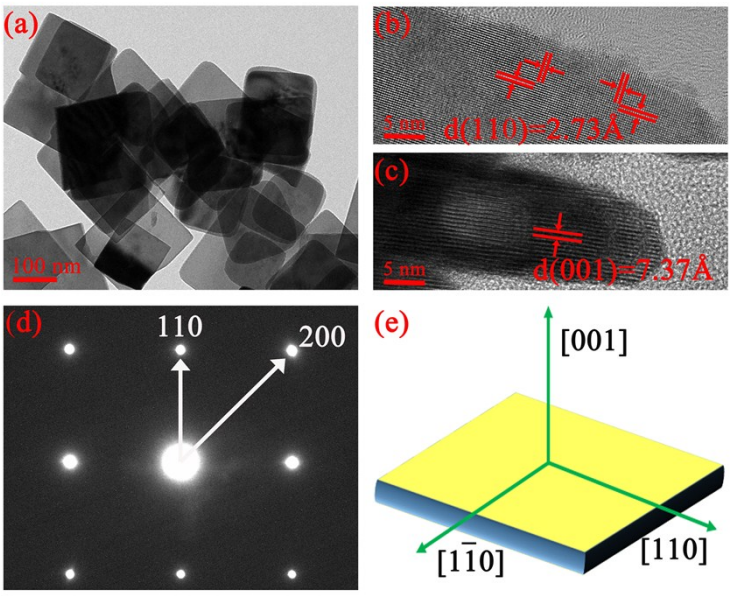


**Figure S5.** (a) TEM image of BOC. (b) HRTEM image taken from the top face of BOC. (c) HRTEM image taken from the side face of BOC. (d) The selected-area electron diffraction (SAED) pattern taken from the top face of BOC. (e) Schematic illustration for the crystal orientation of BOC.

The BiOCl nanoplates show a square-like morphology (**Figure S5a**). The lattice fringes taken from the top face show d-spacing of 2.73 Å (**Figure S5b**), which can be assigned to the BiOCl (110). The HRTEM image of a side face shows dspacing of 7.37 Å (**Figure S5c**), corresponding to the (001) lattice fringes. Confirmed by the SAED pattern (**Figure S5d**), the top and bottom surfaces of BiOCl nanoplates are enclosed by (001) facets while the four side faces are (110) facets (**Figure S5e**).

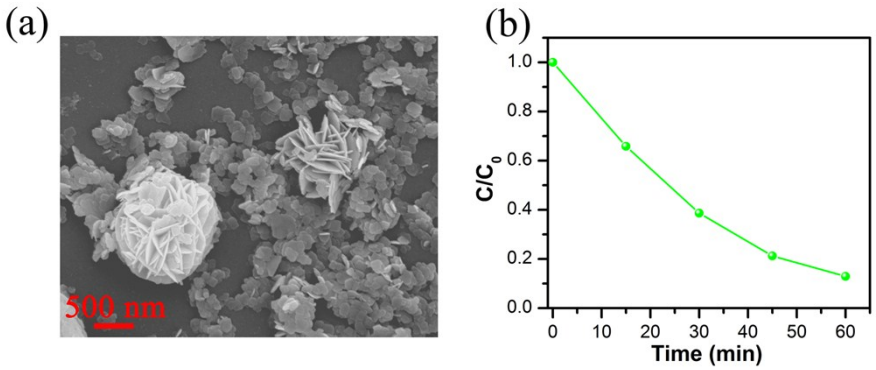


**Figure S6.** SEM (a) and the degradation efficiency under visible light irradiation (b) of BiOCl with iodine doping concentration of 4.21%.

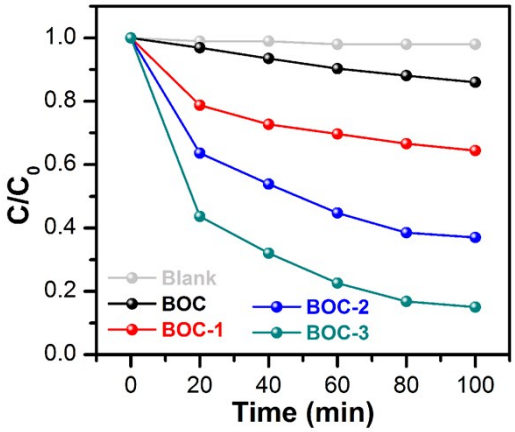


**Figure S7**. The TC-HCl degradation efficiency of BOC, BOC-1, BOC-2 and BOC-3 under visible light irradiation.

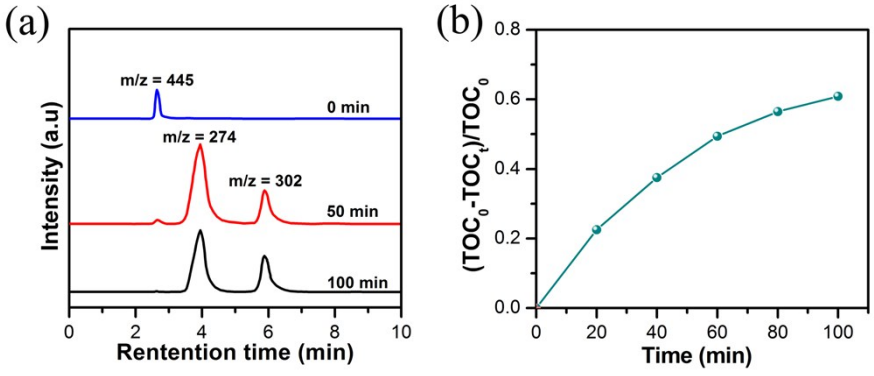


**Figure S8.** LC-MS chromatograms (a) and Total organic carbon (TOC) (b) of the TC-HCl degradation with BOC-3 under visible light irradiation.

As can be seen in **Figure S8a**, the peak of TC-HCl decreases gradually with expanding the radiation time and almost disappears after 100 mins. Meanwhile, two

new peaks with m/z = 302 and 274 in the process of reaction are observed. The TOC change for TC-HCl photodegradation was also tested to reflect the extent of mineralization and the results are depicted in **Figure S8b**. After 100 mins irradiation, the removal efficiency of TOC about BOC-3 sample is approximately 60.89 %, indicating the TC-HCl can be degraded by doped BiOCl under visible light irradiation.

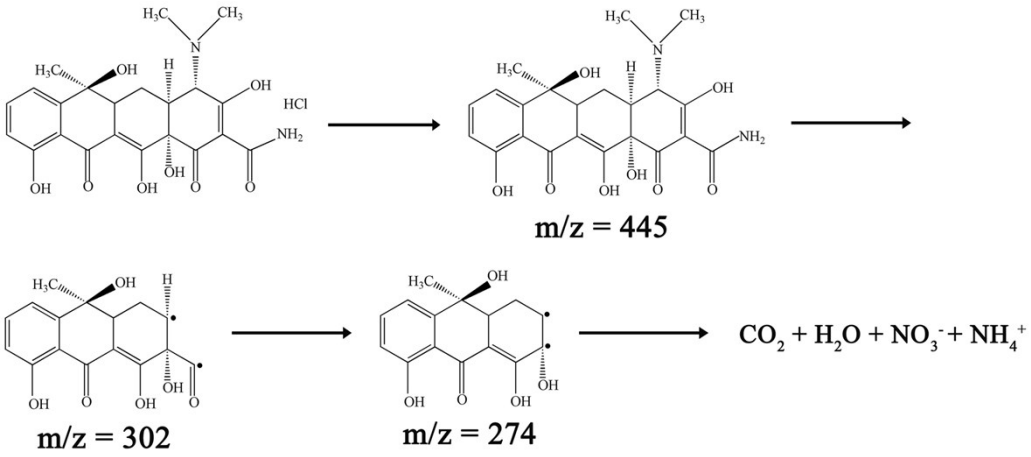


**Figure S9.** The proposed TC-HCl degradation pathway under visible light irradiation.

The proposed TC-HCl degradation pathway: First, the electrons can be excited to CB from VB and the holes generate in VB when BOC-3 sample is irradiated by visible light. Then the generated active species (holes and $\cdot O_2^-$) attack the deprotonated TC-HCl to generate an intermediate 1 (m/z = 302). Subsequently, intermediate 2 (m/z = 274) is produced by shearing carbanyl group in intermediate 1. After further degradation, $CO_2$ or simple organic compounds can be obtained, which can be confirmed by LC-MS chromatograms that the peak intensity at m/z = 274 after 100 mins degradation is smaller than that of 50 mins degradation.

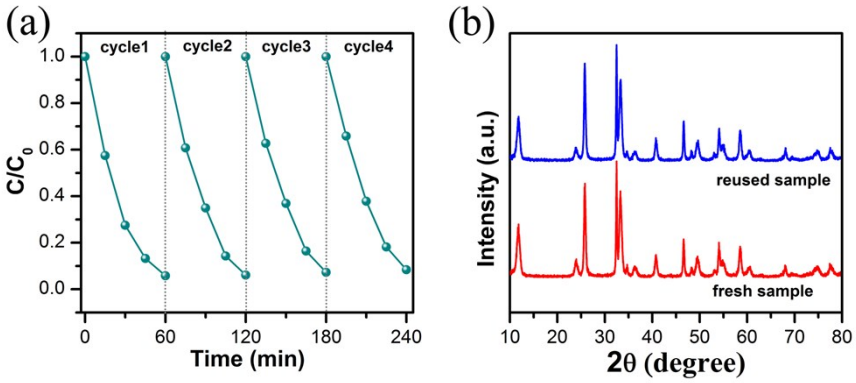


**Figure S10.** (a) The recycling tests of sample in which each cycle lasted 60 mins. (b) XRD of sample before and after photodegradation.

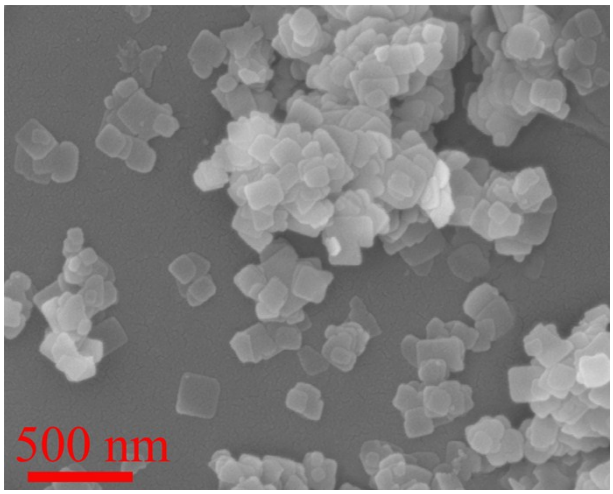


**Figure S11.** SEM image of BOC-3 after photodegradation.

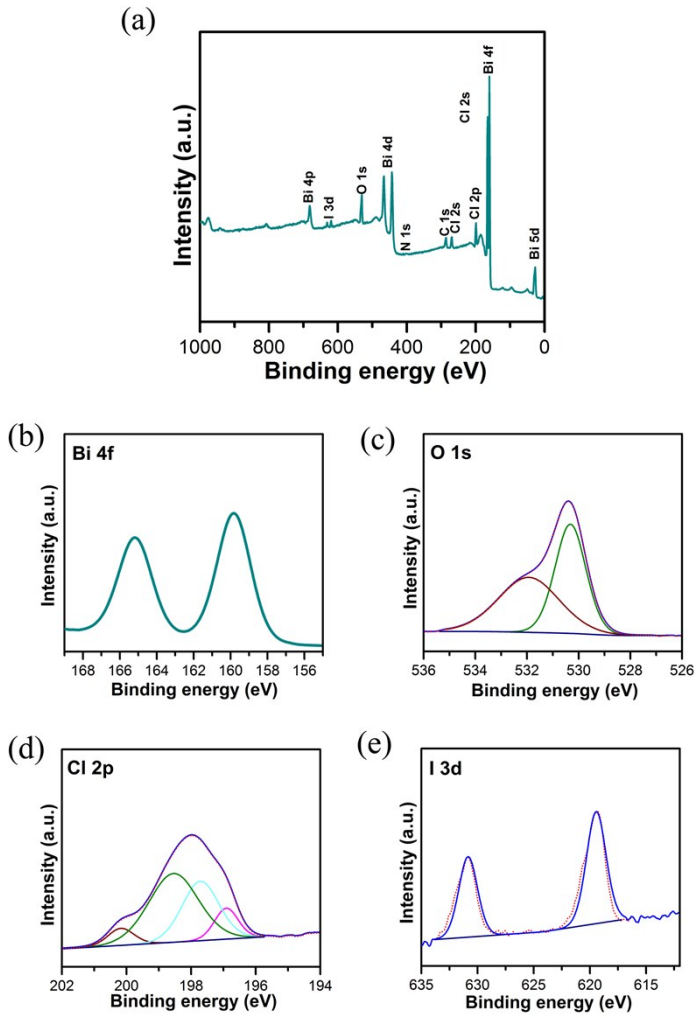


**Figure S12.** XPS of BOC-3 and high-resolution XPS of Bi 4f, O 1s, Cl 2p and I 3d after photodegradation.

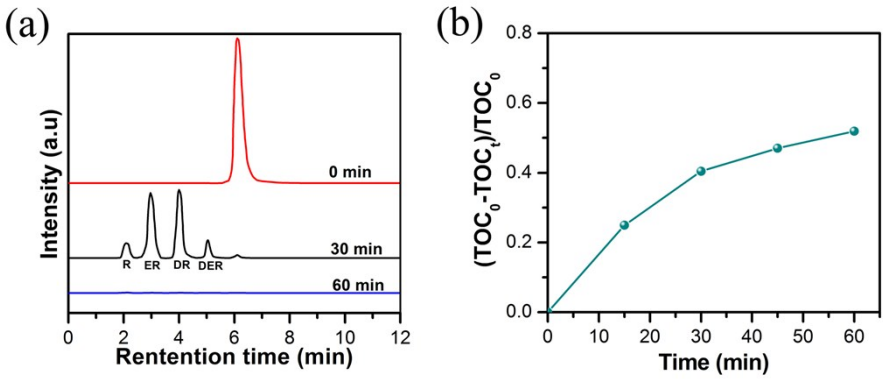


**Figure S13.** LC-MS chromatograms (a) and Total organic carbon (TOC) (b) of the RhB degradation with BOC-3 under visible light irradiation.

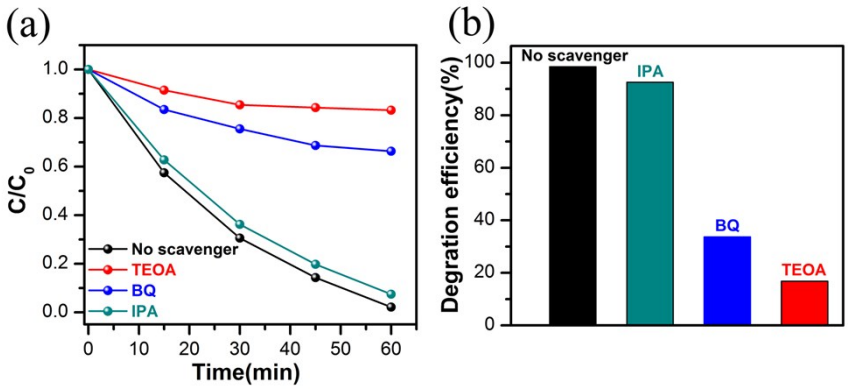


**Figure S14.** Trapping experiments of the active species.

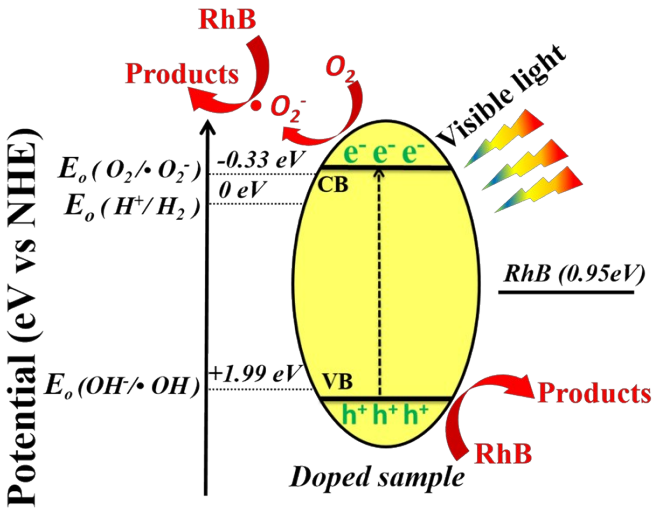


**Figure S15.** The conceivable photodegradation mechanism of RhB over doped BiOCl under visible-light irradiation.

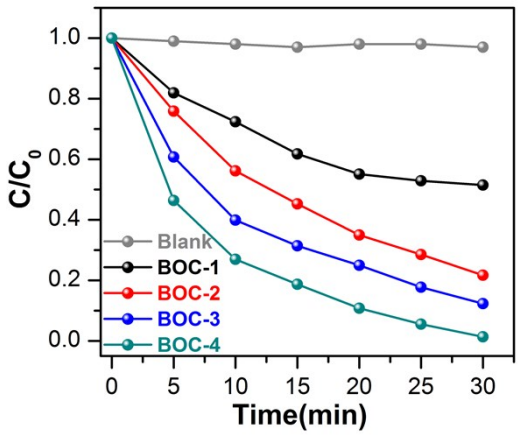


**Figure S16.** The RhB degradation efficiency of BOC, BOC-1, BOC-2 and BOC-3 under UV irradiation.

**Table S1.** Amounts of atoms (%) in BOC, BOC-1, BOC-2 and BOC-3.

| Sample | Amounts of bismuth (%) | Amounts of oxygen (%) | Amounts of chlorine (%) | Amounts of iodine dopant (%) |
|---|---|---|---|---|
| BOC | 32.03 | 32.21 | 35.76 | 0 |
| BOC-1 | 32.01 | 33.03 | 34.24 | 0.72 |
| BOC-2 | 31.99 | 32.41 | 33.79 | 1.81 |
| BOC-3 | 31.36 | 33.29 | 32.30 | 3.05 |

According to the results of XPS, Bi and O atoms of BOC-1, BOC-2 and BOC-3 have the almost same amounts in comparison with that of BOC and the sum of Cl and I amounts in either BOC-1, BOC-2 or BOC-3 is equal to the amount of Cl in BOC. This phenomenon provides a strong evidence of Cl substitution by I. It has been reported that BiOCl possess a layer crystalline structure with the $[Bi_2O_2]^{2+}$ and $Cl^-$ slices stacked together by the nonbonding interaction. Obviously, the weak van der Waals interaction of $Cl^-$ favors its substitution compared to the strong covalent bond between Bi and O.

**Table S2.** Structural information of BOC, BOC-1, BOC-2 and BOC-3.

| Sample | Contents of iodine dopant (%) | Thickness (nm) | In-plane size (nm) | Percentages of (001) facets (%) | specific surface areas ($m^2/g$) |
|---|---|---|---|---|---|
| BOC | 0 | 28-47 | 125-275 | 79.5 | 15.23 |
| BOC-1 | 0.72 | 19-38 | 100-230 | 78.5 | 15.62 |
| BOC-2 | 1.81 | 18-31 | 85-220 | 78.1 | 16.16 |
| BOC-3 | 3.05 | 16-28 | 70-205 | 77.6 | 16.84 |